Superconductors, Quantum Dots, and Spin Entanglement

Mahn-Soo Choi[1,2], C. Bruder[1], and Daniel Loss[1]

[1] Department of Physics and Astronomy, Klingelbergstrasse 82, CH-4056 Basel, Switzerland
[2] Korea Institute for Advanced Study, Cheongryangri-dong 207-43, Seoul 130-012, South Korea

Abstract. In this paper, we review a double quantum dot each dot of which is tunnel-coupled to superconducting leads. In the Coulomb blockade regime, a spin-dependent Josephson coupling between two superconductors is induced, as well as an antiferromagnetic Heisenberg exchange coupling between the spins on the double dot which can be tuned by the superconducting phase difference. We show that the correlated spin states—singlet or triplets—on the double dot can be probed via the Josephson current in a dc-SQUID setup. We also briefly review the Andreev entangler, a non-equilibrium setup that provides a source of pairwise entangled electrons.

1 Introduction

In recent years, electronic transport through strongly interacting mesoscopic systems has been the focus of many investigations [1]. In particular, a single quantum dot coupled via tunnel junctions to two non-interacting leads has provided a prototype model to study Coulomb blockade effects and resonant tunneling in such systems. These studies that started in the 1960's [2] have been extended to an Anderson impurity [3] or a quantum dot coupled to superconductors [4,5,6]. In a number of experimental [4] and theoretical [5] papers, the spectroscopic properties of a quantum dot coupled to two superconductors have been studied. Further, an effective dc Josephson effect through strongly interacting regions between superconducting leads has been analyzed [7,8,9,10]. More recently, on the other hand, research on the possibility to control and detect the spin of electrons through their charges has started. In particular in semiconducting nanostructures, it was found that the direct coupling of two quantum dots by a tunnel junction can be used to create entanglement between spins [11], and that such spin correlations can be observed in charge transport experiments [12].

Motivated by these studies we have proposed a new scenario for inducing and detecting spin correlations, viz., coupling a double quantum dot (DD) to superconducting leads by tunnel junctions [13]. It turns out that this connection via a superconductor induces a Heisenberg exchange coupling between the two spins on the DD. Moreover, if the DD is arranged between two superconductors, we obtain a Josephson junction (S-DD-S). The resulting Josephson current depends on the spin state of the DD and can be used to *probe* the spin correlations on the DD [13]. We have also pointed out that such a Josephson junction can be used

R. Haug and H. Schoeller (Eds.): LNP 579, pp. 46–66, 2001.

in principle to distinguish singlet and triplet superconductors. Finally, a double quantum dot connected to a superconductor and to two leads has been proposed as an Andreev entangler, i.e., a device that allows the injection of spin-entangled electrons into two leads [14].

2 One Quantum Dot

As a warm-up, we would like to discuss a single quantum dot coupled to two superconducting leads (for a more detailed treatment see [3]). The geometry of the system is shown in Fig. 1.

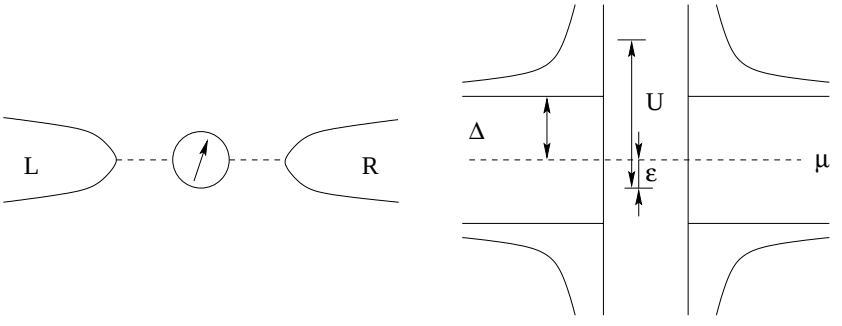

Fig. 1. Left panel: sketch of the superconductor-quantum dot-superconductor (S-D-S) nanostructure. Right panel: schematic representation of the quasiparticle energy spectrum in the superconductors and the energy levels of the quantum dot

The leads are assumed to be conventional singlet superconductors that are described by the BCS Hamiltonian

$$H_S = \sum_{j=L,R} \int_{\Omega_j} \frac{d\mathbf{r}}{\Omega_j} \left\{ \sum_{\sigma=\uparrow,\downarrow} \psi^\dagger_\sigma(\mathbf{r}) h(\mathbf{r}) \psi_\sigma(\mathbf{r}) + \Delta_j(\mathbf{r}) \psi^\dagger_\uparrow(\mathbf{r}) \psi^\dagger_\downarrow(\mathbf{r}) + h.c. \right\} , \quad (1)$$

where Ω_j is the volume of lead j, $h(\mathbf{r}) = (-i\hbar\nabla + \frac{e}{c}\mathbf{A})^2/2m - \mu$, and $\Delta_j(\mathbf{r}) = \Delta_j e^{-i\phi_j(\mathbf{r})}$ is the pair potential. For simplicity, we assume identical leads with same chemical potential μ, and $\Delta_L = \Delta_R = \Delta$. The quantum dot is modeled as a localized level ϵ with strong on-site Coulomb repulsion U, described by the Hamiltonian

$$H_D = -\epsilon \sum_\sigma d^\dagger_{n\sigma} d_{n\sigma} + U d^\dagger_{n\uparrow} d_{n\uparrow} d^\dagger_{n\downarrow} d_{n\downarrow} , \quad (2)$$

where $\epsilon > 0$. U is typically given by the charging energy of the dot, and we have assumed that the level spacing of the dot is $\sim U$ (which is the case for small GaAs dots [1]), so that we need to retain only one energy level in H_D. Finally,

the dot is coupled (see Fig. 1) to the superconducting leads, described by the tunneling Hamiltonian

$$H_T = \sum_{j,\sigma} \left[t \exp(-i\frac{\pi}{\Phi_0} \int_{\mathbf{r}}^{\mathbf{r}_j} d\mathbf{l} \cdot \mathbf{A}) \psi_\sigma^\dagger(\mathbf{r}_j) d_\sigma + h.c. \right] , \tag{3}$$

where $\mathbf{r}_j$ is the point on the lead j closest to the dot. Here, $\Phi_0 = hc/2e$ is the superconducting flux quantum.

Since the low-energy states of the whole system are well separated by the superconducting gap Δ as well as the strong Coulomb repulsion U ($\Delta, \epsilon \ll U - \epsilon$), it is sufficient to consider an effective Hamiltonian on the reduced Hilbert space consisting of singly occupied levels of the dot and the BCS ground states on the leads. To lowest order in H_T, the effective Hamiltonian is given by [15]

$$H_{\text{eff}} = P\, H_T \left[(E_0 - H_0)^{-1} (1 - P) H_T \right]^3 \, P \, , \tag{4}$$

where P is the projection operator onto the subspace and E_0 is the ground-state energy of the unperturbed Hamiltonian H_0. (The second-order contribution leads to an irrelevant constant). The lowest-order expansion (4) is valid in the limit $\Gamma \ll \Delta, \epsilon$ where $\Gamma = \pi t^2 N(0)$ and $N(0)$ is the normal-state density of states per spin of the leads at the Fermi energy. Thus, we assume that $\Gamma \ll \Delta, \epsilon \ll U - \epsilon$, and temperatures which are less than ϵ (but larger than the Kondo temperature).

The explicit calculation of H_{eff} is a special case of the double-dot situation considered in the next section and is outlined in Appendix B. The result is

$$H_{\text{eff}} = \frac{J_0}{2} \cos(\phi) \, , \tag{5}$$

where ϕ is the phase difference between the two superconductors and J_0 is a *positive* constant given in Eq. (8). In other words, a quantum dot tunnel-coupled to two superconductors is a π-junction, the sign of the the Josephson coupling energy is opposite to that of a simple tunnel junction [2,3].

3 Two Quantum Dots

Now we would like to consider the double-dot (DD) system sketched in Fig. 2: Two quantum dots (a,b), each of which contains one (excess) electron and is connected to two superconducting leads (L, R) by tunnel junctions (indicated by dashed lines). Another realization would be atomic impurities embedded between the grains of a granular superconductor. There is no direct coupling between the two dots. The Hamiltonian describing this system consists of three parts, $H_S + H_{DD} + H_T \equiv H_0 + H_T$. The two quantum dots are modeled as two localized levels ϵ_a and ϵ_b with strong on-site Coulomb repulsion U, described by the Hamiltonian

$$H_D = \sum_{n=a,b} \left[-\epsilon \sum_\sigma d_{n\sigma}^\dagger d_{n\sigma} + U d_{n\uparrow}^\dagger d_{n\uparrow} d_{n\downarrow}^\dagger d_{n\downarrow} \right] , \tag{6}$$

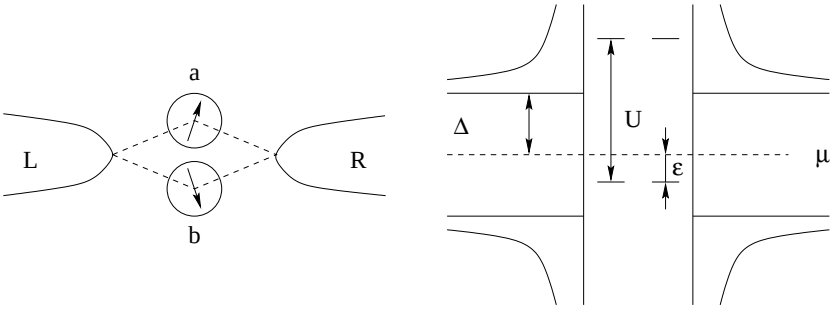

Fig. 2. Left panel: sketch of the superconductor-double quantum dot-superconductor (S-DD-S) nanostructure. Right panel: schematic representation of the quasiparticle energy spectrum in the superconductors and the single-electron levels of the two quantum dots

where we put $\epsilon_a = \epsilon_b = -\epsilon$ ($\epsilon > 0$) for simplicity. As before, we retain only one energy level per dot in H_{DD}. Finally, the DD is coupled *in parallel* (see Fig. 2) to the superconducting leads, described by the tunneling Hamiltonian

$$H_T = \sum_{j,n,\sigma} \left[t \exp(-i\frac{\pi}{\Phi_0} \int_{\mathbf{r}_n}^{\mathbf{r}_{j,n}} d\mathbf{l} \cdot \mathbf{A}) \psi_\sigma^\dagger(\mathbf{r}_{j,n}) d_{n\sigma} + h.c. \right] , \tag{7}$$

where $\mathbf{r}_{j,n}$ is the point on the lead j closest to the dot n. Unless mentioned otherwise, it will be assumed that $\mathbf{r}_{L,a} = \mathbf{r}_{L,b} = \mathbf{r}_L$ and $\mathbf{r}_{R,a} = \mathbf{r}_{R,b} = \mathbf{r}_R$.

Proceeding as before, we calculate the effective Hamiltonian of the system to fourth order in H_T.

There are a number of virtual hopping processes that contribute to the effective Hamiltonian (4), see Fig. 3 for a partial listing and Fig. 5 for a full listing of them. Collecting these various processes, one can get the effective Hamiltonian in terms of the gauge-invariant phase differences ϕ and φ between the superconducting leads and the spin operators $\mathbf{S}_a$ and $\mathbf{S}_b$ of the dots (up to a constant and with $\hbar = 1$)

$$\begin{aligned} H_{\text{eff}} &= J_0 \cos(\pi f_{AB}) \cos(\phi - \pi f_{AB}) \\ &+ \left[(2J_0 + J)(1 + \cos\varphi) + 2J_1(1 + \cos \pi f_{AB}) \right] \left[\mathbf{S}_a \cdot \mathbf{S}_b - 1/4 \right] . \end{aligned} \tag{8}$$

Here $f_{AB} = \Phi_{AB}/\Phi_0$ and Φ_{AB} is the Aharonov-Bohm (AB) flux threading through the closed loop indicated by the dashed lines in Fig. 2. One should be careful to define *gauge-invariant* phase differences ϕ and φ in (8). The phase difference ϕ is defined as usual [16] by

$$\phi = \phi_L(\mathbf{r}_L) - \phi_R(\mathbf{r}_R) - \frac{2\pi}{\Phi_0} \int_{\mathbf{r}_R}^{\mathbf{r}_L} d\ell_a \cdot \mathbf{A} , \tag{9}$$

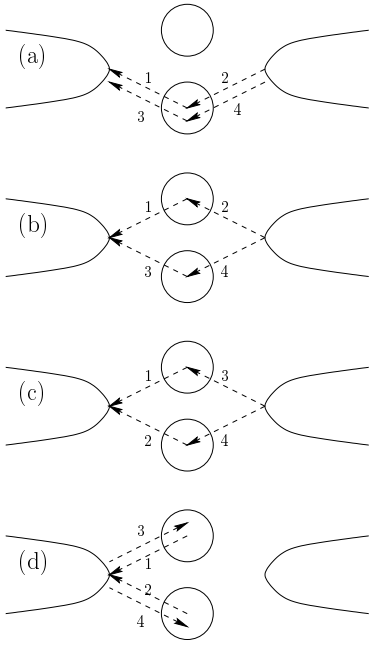

Fig. 3. Partial listing of virtual tunneling processes contributing to $H_{\rm eff}$, Eq. (4). The numbered arrows indicate the direction and the order of occurrence of the charge transfers. Processes of type (a) and (b) give a contribution proportional to J_0, whereas those of type (c) and (d) give contributions proportional to J. For the complete list, see Fig. 5 in Appendix A

where the integration from $\mathbf{r}_R$ to $\mathbf{r}_L$ runs via dot a (see Fig. 2). The second phase difference, φ, is defined by

$$\varphi = \phi_L(\mathbf{r}_L) - \phi_R(\mathbf{r}_R) - \frac{\pi}{\Phi_0}\int_{\mathbf{r}_R}^{\mathbf{r}_L}(d\ell_a + d\ell_b)\cdot\mathbf{A}\ . \tag{10}$$

The distinction between ϕ and φ, however, is not significant unless one is interested in the effects of an AB flux through the closed loop in Fig. 2 (see Ref. [12] for an example of such effects). The coupling constants appearing in (8) are defined by

$$\begin{aligned} J &= \frac{2\Gamma^2}{\epsilon}\left[\frac{1}{\pi}\int\frac{dx}{f(x)g(x)}\right]^2 \\ J_0 &= \frac{\Gamma^2}{\Delta}\int\frac{dxdy}{\pi^2}\,\frac{1}{f(x)f(y)[f(x)+f(y)]g(x)g(y)} \\ J_1 &= \frac{\Gamma^2}{\Delta}\int\frac{dxdy}{\pi^2}\,\frac{g(x)[f(x)+f(y)]-2\zeta g(y)}{g(x)^2g(y)[g(x)+g(y)][f(x)+f(y)]}\ , \end{aligned} \tag{11}$$

where $\zeta = \epsilon/\Delta$, $f(x) = \sqrt{1+x^2}$, and $g(x) = \sqrt{1+x^2}+\zeta$.

A remarkable feature of Eq. (8) is that a Heisenberg exchange coupling between the spin on dot a and on dot b is induced by the superconductor. This coupling is antiferromagnetic (all J's are positive) and thus favors a singlet ground state of spin a and b. This in turn is a direct consequence of the assumed singlet nature of the Cooper pairs in the superconductor (this is discussed further in the next section). As discussed below, an immediate observable consequence of $H_{\rm eff}$ is a *spin-dependent* Josephson current from the left to right superconducting lead (see Fig. 2) which probes the correlated spin state on the DD.

The various terms in (8) have different magnitudes. In particular, the processes leading to the J_1 term involve quasiparticles only as can be seen from its AB-flux dependence which has period $2\Phi_0$. In the limits we will consider below, this J_1 term is small and can be neglected.

In the limit $\zeta \gg 1$, the main contributions come from processes of the type depicted in Fig. 3 (a) and (b), making $J_0 \approx 0.1(\Gamma^2/\zeta\epsilon)\ln\zeta$ dominant over J and J_1. Thus, Eq. (8) can be reduced to

$$H_{\rm eff} \approx J_0 \cos(\pi f_{AB}) \cos(\phi - \pi f_{AB}) + 2J_0(1+\cos\varphi)\left[\mathbf{S}_a \cdot \mathbf{S}_b - \frac{1}{4}\right] , \qquad (12)$$

up to order $(\ln\zeta)/\zeta$. As can be seen in Fig. 3 (a), the first term in Eq. (12) has the same origin as that in the single-dot case [3]: Each dot separately constitutes an effective Josephson junction with coupling energy $-J_0/2$ (i.e. π-junction) between the two superconductors. The two resulting junctions form a dc SQUID, leading to the total Josephson coupling in the first term of (12). The Josephson coupling in the second term in (12), corresponding to processes of type Fig. 3 (b), depends on the correlated spin states on the double dot: For the singlet state, it gives an ordinary Josephson junction with coupling $2J_0$ and competes with the first term, whereas it vanishes for the triplet states. Although the limit $\Delta \ll \epsilon \ll U - \epsilon$ is not easy to achieve with present-day technology, such a regime is relevant, say, for two atomic impurities embedded between the grains of a granular superconductor.

More interesting and experimentally feasible is the case $\zeta \ll 1$. In this regime, the effective Hamiltonian (8) is dominated by a single term (up to terms of order ζ),

$$H_{\rm eff} \approx J(1+\cos\varphi)\ \left[\mathbf{S}_a \cdot \mathbf{S}_b - \frac{1}{4}\right] , \qquad (13)$$

with $J \approx 2\Gamma^2/\epsilon$. The processes of type Fig. 3 (b) and (c) give rise to (13). Below we will propose an experimental setup based on (13).

Before proceeding, we digress briefly on the dependence of J on the contact points. Unlike the processes of type Fig. 3 (a), those of types Fig. 3 (b), (c), and (d) depend on $\delta r_L = |\mathbf{r}_{L,a} - \mathbf{r}_{L,b}|$ and $\delta r_R = |\mathbf{r}_{R,a} - \mathbf{r}_{R,b}|$, see the remark below Eq. (7). For the tunneling Hamiltonian (7), one gets (putting $\delta r = \delta r_L = \delta r_R$)

$$J(\delta r) = \frac{8t^4}{\epsilon}\left|\int_0^\infty \frac{d\omega}{2\pi}\ \frac{F^R(\delta r,\omega) - F^A(\delta r,\omega)}{\omega+\epsilon}\right|^2 , \qquad (14)$$

where $F^{R/A}(\mathbf{r},\omega)$ is the Fourier transform of the Green's function in the superconductors, $F^{R/A}(\mathbf{r},t) = \mp i\Theta(\pm t)\langle\{\psi_\uparrow(\mathbf{r},t),\psi_\downarrow(0,0)\}\rangle$. We note that the phase difference φ in (8) should now be defined with respect to the phase $\phi_j(\mathbf{r}_{j,a},\mathbf{r}_{j,b})$ of the function $F_j^R(\mathbf{r}_{j,a},\mathbf{r}_{j,b}) - F_j^A(\mathbf{r}_{j,a},\mathbf{r}_{j,b})$ on the lead j, see the definition below (8). In the limit $\varepsilon \ll \Delta \ll \mu$, we find $J(\delta r) \approx J(0)e^{-2\delta r/\xi}\sin^2(k_F\delta r)/(k_F\delta r)^2$ up to order $1/k_F\xi$, with k_F the Fermi wave vector in the leads. Hence, the exchange coupling constant is exponentially suppressed if δr exceeds the superconducting coherence length ξ, and there is an additional suppression factor $1/(k_F\delta r)^2$.

4 Probing the Pairing Symmetry of the Superconducting Leads

In the previous section, the superconducting leads were assumed to be conventional BCS superconductors. The discovery of unconventional superconductivity in the heavy-fermion superconductor UPt_3 as well as the high-temperature superconductor $YBa_2Cu_3O_7$ has given a new impetus to the theoretical study of unconventional superconductors. These systems are characterized by an order parameter that is different from the symmetry of the underlying lattice. The order parameter has a nontrivial structure in k-space, usually accompanied by points or lines of zeroes in the gap. Also, the pairing symmetry in spin space that is of singlet type in conventional BCS superconductors can be of triplet type. This behavior is well-known from the p-wave triplet superfluid ^{3}He [17]. Recently, there has been strong evidence that Sr_2RuO_4 is a p-wave triplet superconductor [18].

If, in the previous section, we had assumed leads consisting of unconventional superconductors with triplet pairing, we would find a *ferromagnetic* exchange coupling favoring a triplet ground state of spin a and b on the DD. Thus, by probing the spin ground state of the dots (e.g. via its magnetic moment) we would have a means to *distinguish singlet from triplet pairing*. The magnetization could be made sufficiently large by extending the scheme from two to N dots or impurities coupled to the superconductor.

5 Probing Spins with a dc-SQUID

We now propose a possible experimental setup to probe the correlations (entanglement) of the spins on the dots, based on the effective model (13). According to (13) the S-DD-S structure can be regarded as a *spin-dependent* Josephson junction. Moreover, this structure can be connected with an ordinary Josephson junction to form a dc-SQUID-like geometry, see Fig. 4. The Hamiltonian of the entire system is then given by

$$H = J[1+\cos(\theta - 2\pi f)]\left(\mathbf{S}_a\cdot\mathbf{S}_b - \frac{1}{4}\right) + \alpha J(1-\cos\theta)\ , \tag{15}$$

where $f = \Phi/\Phi_0$, Φ is the flux threading the SQUID loop, θ is the gauge-invariant phase difference across the auxiliary junction (J'), and $\alpha = J'/J$ with J' being

the Josephson coupling energy of the auxiliary junction. Without restriction we can assume $\alpha > 1$, since J' could be adjusted accordingly by replacing the J'-junction by another dc SQUID and flux through it. One immediate consequence of Eq. (15) is that at zero temperature, we can effectively turn on and off the spin exchange interaction: For half-integer flux ($f = 1/2$), singlet and triplet states are degenerate at $\theta = 0$. Even at finite temperatures, where θ is subject to thermal fluctuations, singlet and triplet states are almost degenerate around $\theta = 0$. On the other hand, for integer flux ($f = 0$), the energy of the singlet state is lower by J than that of the triplet states.

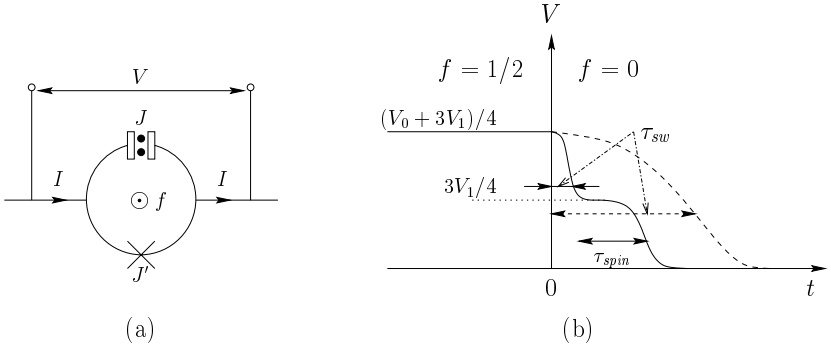

Fig. 4. (**a**) dc-SQUID-like geometry consisting of the S-DD-S structure (filled dots at the top) connected in parallel with another ordinary Josephson junction (cross at the bottom). (**b**) Schematic representation of dc voltage V vs. time when probing the spin correlations of the DD. The flux through the SQUID loop is switched from $f = 1/2$ to $f = 0$ at $t = 0$. Solid line: $\tau_{sw} < \tau_{spin}$. Dashed line: $\tau_{sw} > \tau_{spin}$

This observation allows us to probe directly the spin state on the double dot via a Josephson current across the dc-SQUID-like structure in Fig. 4. The supercurrent through the SQUID-ring is defined as $I_S = (2\pi c/\Phi_0)\partial\langle H\rangle/\partial\theta$, where the brackets refer to a spin expectation value on the DD. Thus, depending on the spin state on the DD we find

$$I_S/I_J = \begin{cases} \sin(\theta - 2\pi f) + \alpha \sin\theta & \text{(singlet)} \\ \alpha \sin\theta & \text{(triplets)} \end{cases} , \tag{16}$$

where $I_J = 2eJ/\hbar$. When the system is biased by a dc current I larger than the spin- and flux-dependent critical current, given by $\max_\theta\{|I_S|\}$, a finite voltage V appears. Then one possible experimental procedure might be as follows (see Fig. 4b). Apply a dc bias current such that $\alpha I_J < I < (\alpha + 1)I_J$. Here, αI_J is the critical current of the triplet states, and $(\alpha + 1)I_J$ the critical current of the singlet state at $f = 0$, see (16). Initially prepare the system in an equal mixture of singlet and triplet states by tuning the flux around $f = 1/2$. (With electron g-factors $g \sim 0.5$–20 the Zeeman splitting on the dots is usually small

compared with k_BT and can thus be ignored.) The dc voltage measured in this mixture will be given by $(V_0 + 3V_1)/4$, where $V_0(V_1) \sim 2\Delta/e$ is the (current-dependent) voltage drop associated with the singlet (triplet) states. At a later time $t = 0$, the flux is switched off (i.e. $f = 0$), with I being kept fixed. The ensuing time evolution of the system is characterized by three time scales: the time $\tau_{coh} \sim \max\{1/\Delta, 1/\Gamma\} \sim 1/\Gamma$ it takes to establish coherence in the S-DD-S junction, the spin relaxation time τ_{spin} on the dot, and the switching time τ_{sw} to reach $f = 0$. We will assume $\tau_{coh} \ll \tau_{spin}, \tau_{sw}$, which is not unrealistic in view of measured spin decoherence times in GaAs exceeding 100ns [19]. If $\tau_{sw} < \tau_{spin}$, the voltage is given by $3V_1/4$ for times less than τ_{spin}, i.e. the singlet no longer contributes to the voltage. For $t > \tau_{spin}$ the spins have relaxed to their ground (singlet) state, and the voltage vanishes. One therefore expects steps in the voltage versus time (solid curve in Fig. 4b). If $\tau_{spin} < \tau_{sw}$, a broad transition region of the voltage from the initial value to 0 will occur (dashed line in Fig. 4b).

Another experimental setup would be to use an rf-SQUID geometry, i.e., to embed the S-DD-S structure into a superconducting ring [16]. However, to operate such a device, ac fields are necessary, and the sensitivity is not as good as for the dc-SQUID geometry.

To our knowledge, there are no experimental reports on quantum dots coupled to superconductors. However, hybrid systems consisting of superconductors (e.g., Al or Nb) and 2DES (InAs and GaAs) have been investigated by a number of groups [20]. Taking the parameters of those materials, a rough estimate leads to a coupling energy J in Eqs. (13) or (15) of about $J \sim 0.05$–0.5K. This corresponds to a critical current scale of $I_J \sim 5$–50nA.

6 Andreev Entangler

Up to now, we have considered equilibrium phenomena. Recently, a system consisting of a double quantum dot coupled to a superconductor on one side and to separate leads on the other side has been proposed as a source of entangled electrons [14]. This entangler is a *non-equilibrium* device that can create pairwise spin-entangled electrons and provide coherent injection by an Andreev process into different dots which are tunnel-coupled to leads, leading to a current

$$I_1 = \frac{4e\gamma_S^2}{\gamma}\left[\frac{\sin(k_F\delta r)}{k_F\delta r}\right]^2 \exp\{-\frac{2\delta r}{\pi\xi}\}\,. \tag{17}$$

Here, γ_S is the tunneling rate between the superconductor and the dots, γ the tunneling rate between the dots and the leads, and δr was defined around Eq. (14).

The unwanted process of both electrons tunneling into the same leads can be suppressed by increasing the Coulomb repulsion on the quantum dot, and its current is given by

$$I_2 = \frac{2e\gamma_S^2\gamma}{\mathcal{E}^2}, \qquad \frac{1}{\mathcal{E}} = \frac{1}{\pi\Delta} + \frac{1}{U}\,. \tag{18}$$

These relations are valid if $\Delta, U > \Delta\mu > \gamma, k_B T$, and $\gamma > \gamma_S$, where $\Delta\mu$ is the bias voltage between the superconductor and the leads. Also, the single-particle level spacing of both dots is assumed to be larger than $\Delta\mu$.

The ratio of currents of these two competing processes is given by

$$\frac{I_1}{I_2} = \frac{2\mathcal{E}^2}{\gamma^2} \left[\frac{\sin(k_F \delta r)}{k_F \delta r}\right]^2 \exp\{-\frac{2\delta r}{\pi\xi}\}\,. \tag{19}$$

From this ratio we see that the desired regime with I_1 dominating I_2 is obtained when $\mathcal{E}/\gamma > k_F \delta r$, and $\delta r < \xi$. We would like to emphasize that the relative suppression of I_2 (as well as the absolute value of the current I_1) is maximized by working around the resonances $\epsilon_l \simeq \mu_S = 0$. It was shown that there exists a regime of experimental interest where the entangled current shows a resonance and assumes a finite value with both partners of the singlet being in different leads but having the same orbital energy. This entangler then satisfies the necessary requirements needed to detect the spin entanglement via transport and noise measurements [12].

Another effect discussed in [14] are flux-dependent oscillations of the current in an Aharonov-Bohm loop. For this let us consider now a setup where the two leads 1 and 2 are connected such that they form an Aharonov-Bohm loop, where the electrons are injected from the left via the superconductor, traversing the upper (lead 1) and lower (lead 2) arm of the loop before they rejoin to interfere and then exit into the same lead, where the current is then measured as a function of varying flux Φ. It is straightforward to analyze this setup. The total flux-dependent Aharonov-Bohm current I_{AB} is found to be [14]

$$I_{AB} = \sqrt{8 I_1 I_2} F(\epsilon_l) \cos(\Phi/2\Phi_0) + I_2 \cos(\Phi/\Phi_0)\,, \tag{20}$$

$$F(\epsilon_l) = \frac{\epsilon_l}{\sqrt{\epsilon_l^2 + (\gamma_L/2)^2}}\,, \tag{21}$$

where, for simplicity, we have assumed that $\epsilon_1 = \epsilon_2 = \epsilon_l$, and $\gamma_1 = \gamma_2 = \gamma_L$. Here, the first term (different leads) is periodic in $2\Phi_0 = h/e$ like for single-electron Aharonov-Bohm interference effects, while the second one (same leads) is periodic in the superconducting flux quantum Φ_0, describing thus the interference of two coherent electrons (similar single- and two-particle Aharonov-Bohm effects occur in the Josephson current through an Aharonov-Bohm loop, see the previous sections and [13]). It is clear from Eq. (20) that the h/e oscillation comes from the interference between a contribution where the two electrons travel through different arms with contributions where the two electrons travel through the same arm. Both Aharonov-Bohm oscillations with period h/e, and $h/2e$, vanish with decreasing I_2, i.e. with increasing on-site repulsion U and/or gap Δ. However, their relative weight is given by $\sqrt{I_1/I_2}$, implying that the $h/2e$ oscillations vanish faster than the h/e ones. This behavior is quite remarkable since it opens up the possibility to tune down the unwanted leakage process $\sim I_2 \cos(\Phi/\Phi_0)$ where two electrons proceed via the same dot/lead by increasing U with a gate voltage applied to the dots. The dominant current contribution

with period h/e comes then from the desired entangled electrons proceeding via different leads. On the other hand, if $\sqrt{I_1/I_2} < 1$, which could become the case e.g. for $k_F \delta r > \mathcal{E}/\gamma$, we are left with $h/2e$ oscillations only. Note that dephasing processes which affect the orbital part suppress I_{AB}. Still, the flux-independent current $I_1 + I_2$ can remain finite and contain electrons which are entangled in spin-space, provided that there is only negligible spin-orbit coupling so that the spin is still a good quantum number.

In conclusion, we have reviewed double quantum dots each dot of which is coupled to superconductors. We have found that in the Coulomb blockade regime the Josephson current from one superconducting lead to the other is different for singlet or triplet states on the double dot. This leads to the possibility to probe the spin states of the dot electrons by measuring a Josephson current. We have discussed the possibility to use a Josephson junction of this type to distinguish between singlet and triplet superconductors. And finally, we have briefly reviewed a non-equilibrium device: the recently proposed Andreev entangler, a source of entangled electrons.

We would like to thank the Swiss National Science Foundation for support.

Appendix A

In this appendix, we would like to enumerate the processes contributing to the effective Hamiltonian, Eq. (4). They are depicted in Fig. 5 and have labels A_1, B_1, B_2, ... E_2.

Each process can be calculated in a straightforward way; as examples, we give the explicit calculations for A_1 and C_1 in the following two appendices. Adding up all of these terms, we get

$$
\begin{aligned}
H_{\text{eff}} = {} & J_0 \cos(\pi f) \cos\phi && \text{Class } A_1 \\
& - Y_1 && \text{Class } B_1 \\
& - (X_1 + Y_2) && \text{Class } B_2 \\
& + J \cos\phi \, [\mathbf{S}_a \cdot \mathbf{S}_b - 1/4] && \text{Class } C_1 \\
& + 2J_0 \cos\phi \, [\mathbf{S}_a \cdot \mathbf{S}_b - 1/4] && \text{Class } C_2 \\
& - 2Y_1 \cos(\pi f) \, [\mathbf{S}_a \cdot \mathbf{S}_b + 1/4] && \text{Class } D_1 \\
& + 2(X_1 + Y_2) \cos(\pi f) \, [\mathbf{S}_a \cdot \mathbf{S}_b + 1/4] && \text{Class } D_2 \\
& + (J + 2X_1 + 2Y_2) \, [\mathbf{S}_a \cdot \mathbf{S}_b - 1/4] && \text{Class } E_1 \\
& + 2J_0 [\mathbf{S}_a \cdot \mathbf{S}_b - 1/4] - 2Y_1 [\mathbf{S}_a \cdot \mathbf{S}_b + 1/4] && \text{Class } E_2
\end{aligned}
$$

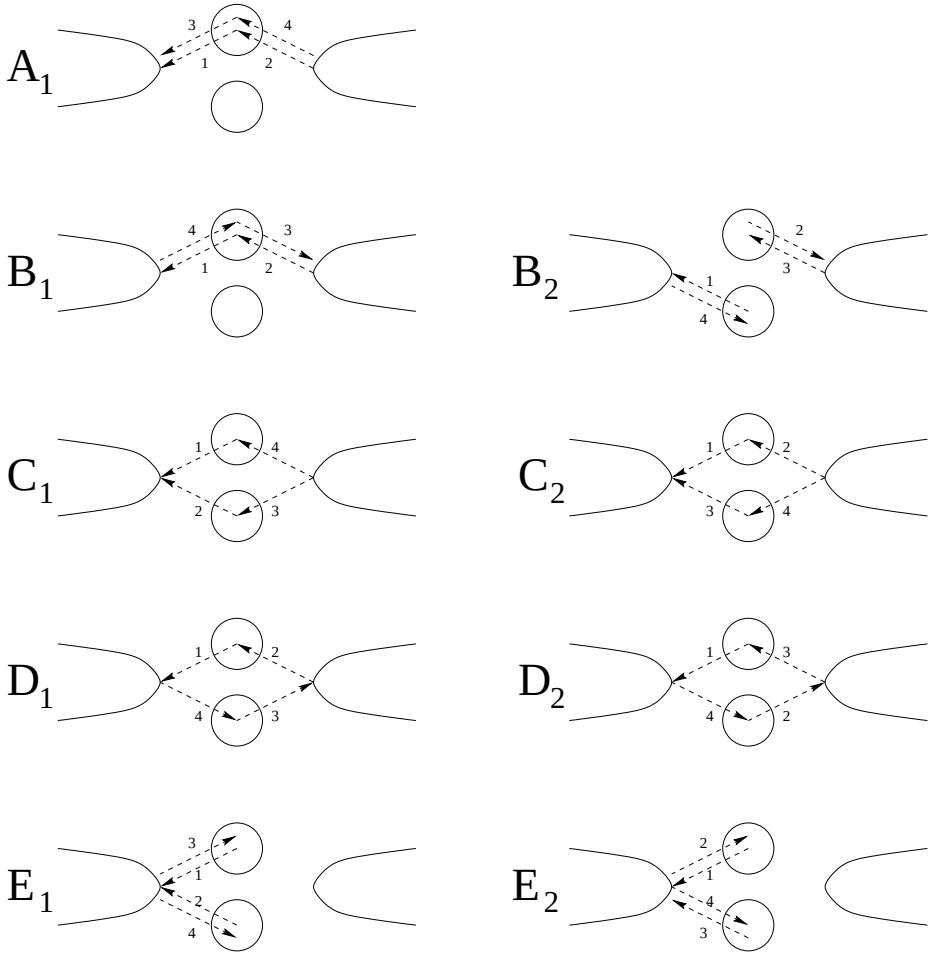

Fig. 5. Processes contributing to the effective Hamiltonian, Eq. (4)

which, after simplification, can be written in the following form:

$$\begin{aligned} H_{\text{eff}} &= J_0 \cos(\pi f) \cos(\varphi - \pi f) \\ &\quad + 2J_0(1 + \cos\phi)\ [\mathbf{S}_a \cdot \mathbf{S}_b - 1/4] \\ &\quad + 2J_1[1 + \cos(\pi f)]\ [\mathbf{S}_a \cdot \mathbf{S}_b - 1/4] \\ &\quad + J(1 + \cos\phi)\ [\mathbf{S}_a \cdot \mathbf{S}_b - 1/4] \\ &\quad + J_1[\cos(\pi f) - 1] - 3Y_1\ . \end{aligned} \tag{22}$$

The coupling constants in these expressions are given by

$$J_0 = \frac{\Gamma^2}{\Delta} \iint \frac{dxdy}{\pi^2} \frac{1}{f(x)f(y)[f(x)+f(y)]g(x)g(y)} \tag{23}$$

$$J_1 = X_1 - X_2 \tag{24}$$

$$J = \frac{2\Gamma^2}{\epsilon} \left[\frac{1}{\pi}\int \frac{dx}{f(x)g(x)}\right]^2 \tag{25}$$

$$X_1 = \frac{\Gamma^2}{\Delta} \iint \frac{dxdy}{\pi^2} \frac{1}{g(x)g(y)[g(x)+g(y)]} \tag{26}$$

$$X_2 = \frac{\Gamma^2}{\Delta} \iint \frac{dxdy}{\pi^2} \frac{2\epsilon/\Delta}{g^2(x)[f(x)+f(y)][g(x)+g(y)]} \equiv Y_1 - Y_2 \tag{27}$$

$$Y_1 = \frac{\Gamma^2}{\Delta} \iint \frac{dxdy}{\pi^2} \frac{1}{[f(x)+f(y)]g^2(x)} \tag{28}$$

$$Y_2 = \frac{\Gamma^2}{\Delta} \iint \frac{dxdy}{\pi^2} \frac{1}{g^2(x)[g(x)+g(y)]} \tag{29}$$

$$f(x) \equiv \sqrt{1+x^2}\,, \quad g(x) \equiv \sqrt{1+x^2} + \epsilon/\Delta\,. \tag{30}$$

They can be derived as follows:

$$\begin{aligned} J_0 &= 4t^4 \sum_{k\in L}\sum_{q\in R} \frac{|u_k v_k^* u_q^* v_q|}{(E_k+\epsilon)(E_q+\epsilon)(E_k+E_q)} \\ &= t^4 \sum_{kq} \frac{|\Delta_L \Delta_R|}{E_k E_q (E_k+E_q)(E_k+\epsilon)(E_q+\epsilon)} \end{aligned} \tag{31}$$

$$J_1 = X_1 - X_2 \tag{32}$$

$$J = 8\frac{t^4}{\epsilon}\left|\sum_k \frac{u_k v_k^*}{E_k+\epsilon}\right|^2 = \frac{2t^4}{\epsilon}\left|\sum_k \frac{\Delta^*}{E_k(E_k+\epsilon)}\right|^2 \tag{33}$$

$$\begin{aligned} X_1 &= 4t^4 \sum_{kq} \frac{|u_k|^2|u_q|^2}{(E_k+\epsilon)(E_q+\epsilon)(E_k+E_q+2\epsilon)} \\ &= t^4 \sum_{kq} \frac{(E_k+\xi_k)(E_q+\xi_q)}{E_k E_q (E_k+\epsilon)(E_q+\epsilon)(E_k+E_q+2\epsilon)} \end{aligned} \tag{34}$$

$$X_2 = Y_1 - Y_2 = 4t^2 \sum_{kq} \frac{2\epsilon|u_k|^2|v_k|^2}{(E_k+\epsilon)^2(E_k+E_q)(E_k+E_q+2\epsilon)} \tag{35}$$

$$Y_1 = 4t^4 \sum_{kp} \frac{|u_k|^2|v_p|^2}{(E_k+\epsilon)^2(E_k+E_q)} = t^4 \sum_{kp} \frac{(E_k+\xi_k)(E_p-\xi_p)}{E_k E_p (E_k+E_q)(E_k+\epsilon)^2} \tag{36}$$

$$Y_2 = 4t^4 \sum_{kq} \frac{|u_k|^2 |u_q|^2}{(E_k+\epsilon)^2 (E_k+E_q+2\epsilon)} = t^4 \sum_{kq} \frac{(E_k+\xi_k)(E_q+\xi_q)}{E_k E_q (E_k+\epsilon)^2 (E_k+E_q+2\epsilon)} \,. \quad (37)$$

More explicitly, with $\zeta = \epsilon/\Delta$, we obtain

$$\begin{aligned} \frac{X_1}{|\Delta|} &= \frac{t^4}{|\Delta|^4} \left[N(0)|\Delta|\right]^2 \\ &\quad \times \int \frac{dxdy\ (\sqrt{1+x^2}+x)(\sqrt{1+y^2}+y)}{\sqrt{1+x^2}(\sqrt{1+x^2}+|\zeta|)\sqrt{1+y^2}(\sqrt{1+y^2}+|\zeta|)(\sqrt{1+x^2}+\sqrt{1+y^2}+|\zeta|)} \\ &= \frac{t^4}{|\Delta|^4} \left[N(0)|\Delta|\right]^2 \int \frac{dxdy}{(\sqrt{1+x^2}+|\zeta|)(\sqrt{1+y^2}+|\zeta|)(\sqrt{1+x^2}+\sqrt{1+y^2}+2|\zeta|)} \end{aligned} \quad (38)$$

$$\begin{aligned} \frac{Y_2}{|\Delta|} &= \frac{t^4}{|\Delta|^4} \left[N(0)|\Delta|\right]^2 \\ &\quad \times \int \frac{dxdy\ (\sqrt{1+x^2}+x)(\sqrt{1+y^2}+y)}{\sqrt{1+x^2}(\sqrt{1+x^2}+|\zeta|)^2\sqrt{1+y^2}(\sqrt{1+x^2}+\sqrt{1+y^2}+|\zeta|)} \\ &= \frac{t^4}{|\Delta|^4} \left[N(0)|\Delta|\right]^2 \int \frac{dxdy}{(\sqrt{1+x^2}+|\zeta|)^2(\sqrt{1+x^2}+\sqrt{1+y^2}+2|\zeta|)} \,. \end{aligned} \quad (39)$$

Appendix B

Here, we would like to evaluate explicitly the contribution of process A_1 (see Fig. 5) to the effective Hamiltonian.

Below, L and U denotes the lower and upper dot. The states that we consider have the form $|G;\sigma_a,\sigma_b;G\rangle$, where σ_a, σ_b denotes the spin states of the dots and G is the BCS ground state of the superconductors. In these calculations, we have retained the $\mathbf{k}$-dependence of the tunneling matrix elements; they are denoted e.g. t_{ka} for the tunneling to dot a. In the end, we set $t_{ka} = t$.

$$|G;\uparrow,\downarrow;G\rangle = d^\dagger_{a\uparrow} d^\dagger_{b\downarrow} |G;0,0;G\rangle$$

$$= d^\dagger_{a\uparrow} d^\dagger_{b\downarrow} \prod_{\mathbf{k}} \left(u_{\mathbf{k}} + v_{\mathbf{k}} c^\dagger_{\mathbf{k}\uparrow} c^\dagger_{-\mathbf{k}\downarrow}\right) \prod_{\mathbf{q}} \left(u_{\mathbf{q}} + v_{\mathbf{q}} c^\dagger_{\mathbf{q}\uparrow} c^\dagger_{-\mathbf{q}\downarrow}\right) |0;0,0;0\rangle$$

$$\xrightarrow{H_T} \sum_{\mathbf{k}} t_{ka} u_{\mathbf{k}}\, \gamma^\dagger_{\mathbf{k}0} d_{a\uparrow}\, d^\dagger_{a\uparrow} d^\dagger_{b\downarrow} |G;0,0;G\rangle = \sum_{\mathbf{k}} t_{ka} u_{\mathbf{k}}\, \gamma^\dagger_{\mathbf{k}0} |G;0,\downarrow;G\rangle$$

$$\xrightarrow{\frac{1-P}{H_0}} + \sum_{k\in L} t_{ka} \frac{u_{\mathbf{k}}}{E_{\mathbf{k}} - \epsilon}\, \gamma^\dagger_{\mathbf{k}0} |G;0,\downarrow;G\rangle$$

$$\begin{aligned}
\xrightarrow{H_T} &+ \sum_{q\in R} t^*_{qa} v_{\mathbf{q}}\, d^\dagger_{a\uparrow}\gamma^\dagger_{\mathbf{q}1} \sum_{k\in L} t_{ka}\frac{u_{\mathbf{k}}}{E_{\mathbf{k}}-\epsilon}\,\gamma^\dagger_{\mathbf{k}0}\,|G;0,\downarrow;G\rangle \\
&- \sum_{q\in R} t^*_{qa} v_{\mathbf{q}}\, d^\dagger_{a\downarrow}\gamma^\dagger_{\mathbf{q}0} \sum_{k\in L} t_{ka}\frac{u_{\mathbf{k}}}{E_{\mathbf{k}}-\epsilon}\,\gamma^\dagger_{\mathbf{k}0}\,|G;0,\downarrow;G\rangle \\
= &+ \sum_{k\in L}\sum_{q\in R} t_{ka}t^*_{qa}\frac{u_{\mathbf{k}}v_{\mathbf{q}}}{E_{\mathbf{k}}-\epsilon}\,\gamma^\dagger_{\mathbf{q}1}\gamma^\dagger_{\mathbf{k}0}\,d^\dagger_{a\uparrow}\,|G;0,\downarrow;G\rangle \\
&- \sum_{k\in L}\sum_{q\in R} t_{ka}t^*_{qa}\frac{u_{\mathbf{k}}v_{\mathbf{q}}}{E_{\mathbf{k}}-\epsilon}\,\gamma^\dagger_{\mathbf{q}0}\gamma^\dagger_{\mathbf{k}0}\,d^\dagger_{a\downarrow}\,|G;0,\downarrow;G\rangle
\end{aligned}$$

$$\begin{aligned}
\xrightarrow{\frac{1-P}{H_0}} &+ \sum_{k\in L}\sum_{q\in R} t_{ka}t^*_{qa}\frac{u_{\mathbf{k}}v_{\mathbf{q}}}{(E_{\mathbf{k}}-\epsilon)(E_{\mathbf{k}}+E_{\mathbf{q}})}\,\gamma^\dagger_{\mathbf{q}1}\gamma^\dagger_{\mathbf{k}0}\,d^\dagger_{a\uparrow}\,|G;0,\downarrow;G\rangle \\
&- \sum_{k\in L}\sum_{q\in R} t_{ka}t^*_{qa}\frac{u_{\mathbf{k}}v_{\mathbf{q}}}{(E_{\mathbf{k}}-\epsilon)(E_{\mathbf{k}}+E_{\mathbf{q}})}\,\gamma^\dagger_{\mathbf{q}0}\gamma^\dagger_{\mathbf{k}0}\,d^\dagger_{a\downarrow}\,|G;0,\downarrow;G\rangle
\end{aligned}$$

$$\begin{aligned}
\xrightarrow{H_T} &+ \sum_{\mathbf{l}\in L} t_{la}u_{\mathbf{l}}\gamma^\dagger_{\mathbf{l}0}d_{a\uparrow} \sum_{k\in L}\sum_{q\in R} t_{ka}t^*_{qa}\frac{u_{\mathbf{k}}v_{\mathbf{q}}}{(E_{\mathbf{k}}-\epsilon)(E_{\mathbf{k}}+E_{\mathbf{q}})}\,\gamma^\dagger_{\mathbf{q}1}\gamma^\dagger_{\mathbf{k}0}\,d^\dagger_{a\uparrow}\,|G;0,\downarrow;G\rangle \\
&+ \sum_{\mathbf{l}\in L} t_{la}u_{\mathbf{l}}\gamma^\dagger_{\mathbf{l}1}d_{a\downarrow}\,(-1)\sum_{k\in L}\sum_{q\in R} t_{ka}t^*_{qa}\frac{u_{\mathbf{k}}v_{\mathbf{q}}}{(E_{\mathbf{k}}-\epsilon)(E_{\mathbf{k}}+E_{\mathbf{q}})}\,\gamma^\dagger_{\mathbf{q}0}\gamma^\dagger_{\mathbf{k}0}\,d^\dagger_{a\downarrow}\,|G;0,\downarrow;G\rangle \\
&- \sum_{\mathbf{l}\in L} t_{la}v^*_{\mathbf{l}}\gamma_{\mathbf{l}0}d_{a\downarrow}\,(-1)\sum_{k\in L}\sum_{q\in R} t_{ka}t^*_{qa}\frac{u_{\mathbf{k}}v_{\mathbf{q}}}{(E_{\mathbf{k}}-\epsilon)(E_{\mathbf{k}}+E_{\mathbf{q}})}\,\gamma^\dagger_{\mathbf{q}0}\gamma^\dagger_{\mathbf{k}0}\,d^\dagger_{a\downarrow}\,|G;0,\downarrow;G\rangle \\
= &+ \sum_{kl\in L}\sum_{q\in R} t_{ka}t_{la}t^*_{qa}\frac{u_{\mathbf{k}}u_{\mathbf{l}}v_{\mathbf{q}}}{(E_{\mathbf{k}}-\epsilon)(E_{\mathbf{k}}+E_{\mathbf{q}})}\,\gamma^\dagger_{\mathbf{l}0}\gamma^\dagger_{\mathbf{q}1}\gamma^\dagger_{\mathbf{k}0}\;|G;0,\downarrow;G\rangle \\
&- \sum_{kl\in L}\sum_{q\in R} t_{ka}t_{la}t^*_{qa}\frac{u_{\mathbf{k}}u_{\mathbf{l}}v_{\mathbf{q}}}{(E_{\mathbf{k}}-\epsilon)(E_{\mathbf{k}}+E_{\mathbf{q}})}\,\gamma^\dagger_{\mathbf{l}1}\gamma^\dagger_{\mathbf{q}0}\gamma^\dagger_{\mathbf{k}0}\;|G;0,\downarrow;G\rangle \\
&- \sum_{k\in L}\sum_{q\in R} t^2_{ka}t^*_{qa}\frac{u_{\mathbf{k}}v^*_{\mathbf{k}}v_{\mathbf{q}}}{(E_{\mathbf{k}}-\epsilon)(E_{\mathbf{k}}+E_{\mathbf{q}})}\,\gamma^\dagger_{\mathbf{q}0}\;|G;0,\downarrow;G\rangle\;.
\end{aligned}$$

Here the contributions of the first and second terms will vanish because one cannot get the final BCS ground state for the SC from these states.

$$\xrightarrow{\frac{1-P}{H_0}} -\sum_{k\in L}\sum_{q\in R} t^2_{ka}t^*_{qa}\frac{u_{\mathbf{k}}v^*_{\mathbf{k}}v_{\mathbf{q}}}{(E_{\mathbf{k}}-\epsilon)(E_{\mathbf{k}}+E_{\mathbf{q}})(E_{\mathbf{q}}-\epsilon)}\,\gamma^\dagger_{\mathbf{q}0}\;|G;0,\downarrow;G\rangle$$

$$\begin{aligned}
\xrightarrow{H_T} &+ t^*_{qa}u^*_{\mathbf{q}}d^\dagger_{a\uparrow}\gamma_{\mathbf{q}0}\,(-1)\sum_{k\in L}\sum_{q\in R} t^2_{ka}t^*_{qa}\frac{u_{\mathbf{k}}v^*_{\mathbf{k}}v_{\mathbf{q}}}{(E_{\mathbf{k}}-\epsilon)(E_{\mathbf{k}}+E_{\mathbf{q}})(E_{\mathbf{q}}-\epsilon)}\,\gamma^\dagger_{\mathbf{q}0}\;|G;0,\downarrow;G\rangle \\
= &- \sum_{k\in L}\sum_{q\in R} t_{ka}t_{ka}t^*_{qa}t^*_{qa}\frac{u_{\mathbf{k}}v^*_{\mathbf{k}}u^*_{\mathbf{q}}v_{\mathbf{q}}}{(E_{\mathbf{k}}-\epsilon)(E_{\mathbf{k}}+E_{\mathbf{q}})(E_{\mathbf{q}}-\epsilon)}\;|G;\uparrow,\downarrow;G\rangle \\
= &- t^4 e^{-i4\pi f/4}\sum_{k\in L}\sum_{q\in R}\frac{\Delta^*_L\Delta_R}{4E_k(E_{\mathbf{k}}-\epsilon)E_q(E_{\mathbf{q}}-\epsilon)(E_{\mathbf{k}}+E_{\mathbf{q}})}\;|G;\uparrow,\downarrow;G\rangle \\
= &- \frac{1}{4}J_0 e^{i(\phi-4\pi f/4)}\;|G;\uparrow,\downarrow;G\rangle\;.
\end{aligned}$$

The path which transfers Cooper pairs from the left to the right superconductor contributes the complex conjugate of the above one. On the other hand, the paths through the upper dots have contributions with factor $e^{+i4\pi f/4}$.

Here, it should be noticed that ϕ is *not* gauge invariant. Therefore it is useful to rewrite

$$t_{ka}t_{ka}t^*_{qa}t^*_{qa}\,\Delta^*_L\Delta_R = t^4\exp\left(-i\,2\times\frac{2\pi}{2\Phi_0}\int_R^L d\boldsymbol{\ell}_a\cdot\mathbf{A}\right)\exp[i(\phi_L-\phi_R)] \tag{40}$$

$$= t^4\exp\left[i\left(\phi_L-\phi_R-\frac{2\pi}{\Phi_0}\int_R^L d\boldsymbol{\ell}_a\cdot\mathbf{A}\right)\right] \tag{41}$$

$$\equiv t^4 e^{+i\varphi_a}\ . \tag{42}$$

As the result of this calculation, we obtain

$$H^{(4)}_{A_1} = \frac{J_0}{2}\left[\cos\varphi_a+\cos\varphi_b\right] = J_0\cos(\pi f)\cos(\varphi_b-\pi f)\ , \tag{43}$$

where

$$\theta_n \equiv \phi_L-\phi_R-\frac{2\pi}{\Phi_0}\int_R^L d\boldsymbol{\ell}_n\cdot\mathbf{A}\ . \tag{44}$$

It is interesting to think about the effect discussed above in the following way: Class A_1 processes describe the fact that each quantum dot forms a π-junction between the two superconductors. We thus have two π-junctions linked in a loop as in a dc-SQUID, through which AB flux threads. The total energy for this configuration is given by

$$H^{(1)}_{A_1} = \frac{1}{2}J_0\cos\varphi+\frac{1}{2}J_0\cos(\varphi-2\pi f) = J_0\cos(\pi f)\cos(\varphi-\pi f)\ . \tag{45}$$

Appendix C

Here, we would like to evaluate explicitly the contribution of process C_1 to the effective Hamiltonian. The hopping events labeled 1 to 4 in Fig. 5 can be combined in a different order that have to be considered separately. We distinguish these different "paths" by labels P_i, $i=1,2,...$ and consider the relevant possibilities.

$$\langle G;\uparrow,\downarrow;G|\,H^{(4)}\,|G;\uparrow,\downarrow;G\rangle\begin{cases}4\leftarrow3\leftarrow2\leftarrow1 & :P_1\\ 3\leftarrow4\leftarrow2\leftarrow1 & :P_2\\ 4\leftarrow3\leftarrow1\leftarrow2 & :P_3\\ 3\leftarrow4\leftarrow1\leftarrow2 & :P_4\end{cases}$$

$$\langle G;\downarrow,\uparrow;G|\,H^{(4)}\,|G;\uparrow,\downarrow;G\rangle\begin{cases}4\leftarrow3\leftarrow2\leftarrow1 & :P_5\\ 3\leftarrow4\leftarrow2\leftarrow1 & :P_6\\ 4\leftarrow3\leftarrow1\leftarrow2 & :P_7\\ 3\leftarrow4\leftarrow1\leftarrow2 & :P_8\end{cases}$$

Neither the configuration $|G;\uparrow,\uparrow;G\rangle$ nor $|G;\downarrow,\downarrow;G\rangle$ can gain energy via cotunneling of this type.

Path P_1:

$$|G;\uparrow,\downarrow;G\rangle = d^\dagger_{a\uparrow} d^\dagger_{b\downarrow} |G;0,0;G\rangle$$

$$= d^\dagger_{a\uparrow} d^\dagger_{b\downarrow} \prod_{\mathbf{k}} \left(u_{\mathbf{k}} + v_{\mathbf{k}} c^\dagger_{\mathbf{k}\uparrow} c^\dagger_{-\mathbf{k}\downarrow} \right) \prod_{\mathbf{q}} \left(u_{\mathbf{q}} + v_{\mathbf{q}} c^\dagger_{\mathbf{q}\uparrow} c^\dagger_{-\mathbf{q}\downarrow} \right) |0;0,0;0\rangle$$

$$\xrightarrow{H_T} \sum_{k\in L} t_{ka} u_k \, \gamma^\dagger_{k0} d_{a\uparrow} \, d^\dagger_{a\uparrow} d^\dagger_{b\downarrow} \, |G;0,0;G\rangle = \sum_{k\in L} t_{ka} u_k \, \gamma^\dagger_{k0} d^\dagger_{b\downarrow} \, |G;0,0;G\rangle$$

$$\xrightarrow{\frac{1-P}{H_0}} \sum_{k\in L} t_{ka} \frac{u_k}{E_k - \epsilon} \, \gamma^\dagger_{k0} d^\dagger_{b\downarrow} \, |G;0,0;G\rangle$$

$$\begin{aligned} \xrightarrow{H_T} &+ \sum_{l\in L} t_{lb} u_l \gamma^\dagger_{l1} d_{b\downarrow} \sum_{k\in L} t_{ka} \frac{u_k}{E_k - \epsilon} \, \gamma^\dagger_{k0} d^\dagger_{b\downarrow} \, |G;0,0;G\rangle \\ &+ \sum_{l\in L} t_{lb} v^*_l \gamma_{l0} d_{b\downarrow} \sum_{k\in L} t_{ka} \frac{u_k}{E_k - \epsilon} \, \gamma^\dagger_{k0} d^\dagger_{b\downarrow} \, |G;0,0;G\rangle \\ = &+ \sum_{kl\in L} t_{ka} t_{lb} \frac{u_k u_l}{E_k - \epsilon} \, \gamma^\dagger_{k0} \gamma^\dagger_{l1} \, |G;0,0;G\rangle \\ &+ \sum_{k\in L} t_{kl} t_{lb} \frac{u_k v^*_k}{E_k - \epsilon} \, |G;0,0;G\rangle \end{aligned}$$

$$\begin{aligned} \xrightarrow{\frac{1-P}{H_0}} &+ \sum_{kl\in L} t_{ka} t_{lb} \frac{u_k u_l}{(E_k - \epsilon)(E_k + E_l - 2\epsilon)} \, \gamma^\dagger_{k0} \gamma^\dagger_{l1} \, |G;0,0;G\rangle \\ &+ \sum_{k\in L} t_{ka} t_{lb} \frac{u_k v^*_k}{(E_k - \epsilon)(-2\epsilon)} \, |G;0,0;G\rangle \ . \end{aligned}$$

The first term will be projected out at the end.

$$\begin{aligned} \xrightarrow{H_T} &+ \sum_{p\in R} t^*_{pb} u^*_p d^\dagger_{b\downarrow} \gamma_{p1} \sum_{k\in L} t_{ka} t_{lb} \frac{u_k v^*_k}{(E_k - \epsilon)(-2\epsilon)} \, |G;0,0;G\rangle \\ &- \sum_{p\in R} t^*_{pb} v_p d^\dagger_{b\downarrow} \gamma^\dagger_{p0} \sum_{k\in L} t_{ka} t_{lb} \frac{u_k v^*_k}{(E_k - \epsilon)(-2\epsilon)} \, |G;0,0;G\rangle \\ = &+ \sum_{k\in L} \sum_{p\in R} t_{ka} t_{lb} t^*_{pb} \frac{u_k v^*_k v_p}{(E_k - \epsilon)(-2\epsilon)} \, \gamma^\dagger_{p0} \, d^\dagger_{b\downarrow} \, |G;0,0;G\rangle \end{aligned}$$

$$\xrightarrow{\frac{1-P}{H_0}} + \sum_{k\in L} \sum_{p\in R} t_{ka} t_{lb} t^*_{pb} \frac{u_k v^*_k v_p}{(E_k - \epsilon)(-2\epsilon)(E_p - \epsilon)} \, \gamma^\dagger_{p0} \, d^\dagger_{b\downarrow} \, |G;0,0;G\rangle$$

$$\begin{aligned}
\xrightarrow{H_T} &+ \sum_{q\in R} t^*_{qa} u^*_q d^\dagger_{a\uparrow} \gamma_{q0} \sum_{k\in L}\sum_{p\in R} t_{ka} t_{lb} t^*_{pb} \frac{u_k v^*_k v_p}{(E_k-\epsilon)(-2\epsilon)(E_p-\epsilon)} \gamma^\dagger_{p0} d^\dagger_{b\downarrow} \; |G;0,0;G\rangle \\
&= + \sum_{k\in L}\sum_{p\in R} t_{ka} t_{lb} t^*_{pb} t^*_{pa} \frac{u_k v^*_k u^*_p v_p}{(E_k-\epsilon)(-2\epsilon)(E_p-\epsilon)} d^\dagger_{a\uparrow} d^\dagger_{b\downarrow} \; |G;0,0;G\rangle \\
&= + t^4 \sum_{k\in L}\sum_{p\in R} \frac{u_k v^*_k u^*_p v_p}{(E_k-\epsilon)(-2\epsilon)(E_p-\epsilon)} \; |G;\uparrow,\downarrow;G\rangle \\
&= + \frac{1}{16} J e^{+i\phi} \; |G;\uparrow,\downarrow;G\rangle \; .
\end{aligned}$$

The path which transfers Cooper pairs from the left to the right superconductor contributes the complex conjugate of the above one.

Path P_2:

$$|G;\uparrow,\downarrow;G\rangle = d^\dagger_{a\uparrow} d^\dagger_{b\downarrow} \, |G;0,0;G\rangle$$

$$= d^\dagger_{a\uparrow} d^\dagger_{b\downarrow} \prod_{\mathbf{k}} \left(u_{\mathbf{k}} + v_{\mathbf{k}} c^\dagger_{\mathbf{k}\uparrow} c^\dagger_{-\mathbf{k}\downarrow} \right) \prod_{\mathbf{q}} \left(u_{\mathbf{q}} + v_{\mathbf{q}} c^\dagger_{\mathbf{q}\uparrow} c^\dagger_{-\mathbf{q}\downarrow} \right) |0;0,0;0\rangle$$

$$\xrightarrow{H_T} - t \sum_{k\in L} u_k \, \gamma^\dagger_{k0} d_{a\uparrow} \, d^\dagger_{a\uparrow} d^\dagger_{b\downarrow} \, |G;0,0;G\rangle = -t \sum_{k\in L} u_k \, \gamma^\dagger_{k0} d^\dagger_{b\downarrow} \; |G;0,0;G\rangle$$

$$\xrightarrow[H_0]{1-P} - t \sum_{k\in L} \frac{u_k}{E_k-\epsilon} \, \gamma^\dagger_{k0} d^\dagger_{b\downarrow} \; |G;0,0;G\rangle$$

$$\begin{aligned}
\xrightarrow{H_T} &- t \sum_{l\in L} u_l \gamma^\dagger_{l1} d_{b\downarrow} \, (-t) \sum_{k\in L} \frac{u_k}{E_k-\epsilon} \, \gamma^\dagger_{k0} d^\dagger_{b\downarrow} \; |G;0,0;G\rangle \\
&+ t \sum_{l\in L} v^*_l \gamma_{l0} d_{b\downarrow} \, (-t) \sum_{k\in L} \frac{u_k}{E_k-\epsilon} \, \gamma^\dagger_{k0} d^\dagger_{b\downarrow} \; |G;0,0;G\rangle \\
= &+ t^2 \sum_{kl\in L} \frac{u_k u_l}{E_k-\epsilon} \, \gamma^\dagger_{k0} \gamma^\dagger_{l1} \, |G;0,0;G\rangle \\
&+ t^2 \sum_{k\in L} \frac{u_k v^*_k}{E_k-\epsilon} \; |G;0,0;G\rangle
\end{aligned}$$

$$\begin{aligned}
\xrightarrow[H_0]{1-P} &+ t^2 \sum_{kl\in L} \frac{u_k u_l}{(E_k-\epsilon)(E_k+E_l-2\epsilon)} \, \gamma^\dagger_{k0} \gamma^\dagger_{l1} \, |G;0,0;G\rangle \\
&+ t^2 \sum_{k\in L} \frac{u_k v^*_k}{(E_k-\epsilon)(-2\epsilon)} \; |G;0,0;G\rangle \; .
\end{aligned}$$

The first term will be projected out at the end.

$$\xrightarrow{H_T} -t\sum_{p\in R} v_p d^\dagger_{a\uparrow}\gamma^\dagger_{p1}\,(+t^2)\sum_{k\in L}\frac{u_k v_k^*}{(E_k-\epsilon)(-2\epsilon)}\;|G;0,0;G\rangle$$

$$=+t^3\sum_{k\in L}\sum_{p\in R}\frac{u_k v_k^* v_p}{(E_k-\epsilon)(-2\epsilon)}\,\gamma^\dagger_{p1}\,d^\dagger_{a\uparrow}\;|G;0,0;G\rangle$$

$$\xrightarrow{\frac{1-P}{H_0}} +t^3\sum_{k\in L}\sum_{p\in R}\frac{u_k v_k^* v_p}{(E_k-\epsilon)(-2\epsilon)(E_p-\epsilon)}\,\gamma^\dagger_{p1}\,d^\dagger_{a\uparrow}\;|G;0,0;G\rangle$$

$$\xrightarrow{H_T} -t\sum_{q\in R} u_q^* d^\dagger_{b\downarrow}\gamma_{q1}\,(+t^3)\sum_{k\in L}\sum_{p\in R}\frac{u_k v_k^* v_p}{(E_k-\epsilon)(-2\epsilon)(E_p-\epsilon)}\,\gamma^\dagger_{p1}\,d^\dagger_{a\uparrow}\;|G;0,0;G\rangle$$

$$=+t^4\sum_{k\in L}\sum_{p\in R}\frac{u_k v_k^* u_p^* v_p}{(E_k-\epsilon)(-2\epsilon)(E_p-\epsilon)}\,d^\dagger_{a\uparrow}d^\dagger_{b\downarrow}\;|G;0,0;G\rangle$$

$$=+t^4\sum_{k\in L}\sum_{p\in R}\frac{u_k v_k^* u_p^* v_p}{(E_k-\epsilon)(-2\epsilon)(E_p-\epsilon)}\;|G;\uparrow,\downarrow;G\rangle$$

$$=+\frac{1}{16}Je^{+i\phi}\;|G;\uparrow,\downarrow;G\rangle\;.$$

The path which transfers Cooper pairs from the left to the right superconductor contributes the complex conjugate of the above one.

Path P_5:

$$|G;\uparrow,\downarrow;G\rangle = d^\dagger_{a\uparrow}d^\dagger_{b\downarrow}\,|G;0,0;G\rangle$$

$$=d^\dagger_{a\uparrow}d^\dagger_{b\downarrow}\prod_{\mathbf{k}}\left(u_{\mathbf{k}}+v_{\mathbf{k}}c^\dagger_{\mathbf{k}\uparrow}c^\dagger_{-\mathbf{k}\downarrow}\right)\prod_{\mathbf{q}}\left(u_{\mathbf{q}}+v_{\mathbf{q}}c^\dagger_{\mathbf{q}\uparrow}c^\dagger_{-\mathbf{q}\downarrow}\right)|0;0,0;0\rangle$$

$$\xrightarrow{H_T} -t\sum_{k\in L}u_k\,\gamma^\dagger_{k0}d_{a\uparrow}\,d^\dagger_{a\uparrow}d^\dagger_{b\downarrow}\,|G;0,0;G\rangle=-t\sum_{k\in L}u_k\,\gamma^\dagger_{k0}d^\dagger_{b\downarrow}\;|G;0,0;G\rangle$$

$$\xrightarrow{\frac{1-P}{H_0}} -t\sum_{k\in L}\frac{u_k}{E_k-\epsilon}\,\gamma^\dagger_{k0}d^\dagger_{b\downarrow}\;|G;0,0;G\rangle$$

$$\xrightarrow{H_T} -t\sum_{l\in L}u_l\gamma^\dagger_{l1}d_{b\downarrow}\,(-t)\sum_{k\in L}\frac{u_k}{E_k-\epsilon}\,\gamma^\dagger_{k0}d^\dagger_{b\downarrow}\;|G;0,0;G\rangle$$

$$+t\sum_{l\in L}v_l^*\gamma_{l0}d_{b\downarrow}\,(-t)\sum_{k\in L}\frac{u_k}{E_k-\epsilon}\,\gamma^\dagger_{k0}d^\dagger_{b\downarrow}\;|G;0,0;G\rangle$$

$$=+t^2\sum_{kl\in L}\frac{u_k u_l}{E_k-\epsilon}\,\gamma^\dagger_{k0}\gamma^\dagger_{l1}\,|G;0,0;G\rangle$$

$$+t^2\sum_{k\in L}\frac{u_k v_k^*}{E_k-\epsilon}\;|G;0,0;G\rangle$$

$$\xrightarrow{\frac{1-P}{H_0}} + t^2 \sum_{kl\in L} \frac{u_k u_l}{(E_k-\epsilon)(E_k+E_l-2\epsilon)}\, \gamma^\dagger_{k0}\gamma^\dagger_{l1}\, |G;0,0;G\rangle$$
$$+ t^2 \sum_{k\in L} \frac{u_k v_k^*}{(E_k-\epsilon)(-2\epsilon)}\, |G;0,0;G\rangle \ .$$

The first term will be projected out at the end.

$$\xrightarrow{H_T} - t \sum_{p\in R} u_p^* d^\dagger_{b\uparrow}\gamma_{p0}\, (+t^2) \sum_{k\in L} \frac{u_k v_k^*}{(E_k-\epsilon)(-2\epsilon)}\, |G;0,0;G\rangle$$
$$- t \sum_{p\in R} v_p d^\dagger_{b\uparrow}\gamma^\dagger_{p1}\, (+t^2) \sum_{k\in L} \frac{u_k v_k^*}{(E_k-\epsilon)(-2\epsilon)}\, |G;0,0;G\rangle$$
$$= + t^3 \sum_{k\in L}\sum_{p\in R} \frac{u_k v_k^* v_p}{(E_k-\epsilon)(-2\epsilon)}\, \gamma^\dagger_{p1}\, d^\dagger_{b\uparrow}\, |G;0,0;G\rangle$$

$$\xrightarrow{\frac{1-P}{H_0}} + t^3 \sum_{k\in L}\sum_{p\in R} \frac{u_k v_k^* v_p}{(E_k-\epsilon)(-2\epsilon)(E_p-\epsilon)}\, \gamma^\dagger_{p1}\, d^\dagger_{b\uparrow}\, |G;0,0;G\rangle$$

$$\xrightarrow{H_T} - t \sum_{q\in R} u_q^* d^\dagger_{a\downarrow}\gamma_{q1}\, (+t^3) \sum_{k\in L}\sum_{p\in R} \frac{u_k v_k^* v_p}{(E_k-\epsilon)(-2\epsilon)(E_p-\epsilon)}\, \gamma^\dagger_{p1}\, d^\dagger_{b\uparrow}\, |G;0,0;G\rangle$$
$$= - t^4 \sum_{k\in L}\sum_{p\in R} \frac{u_k v_k^* u_q^* v_p}{(E_k-\epsilon)(-2\epsilon)(E_p-\epsilon)}\, d^\dagger_{a\downarrow} d^\dagger_{b\uparrow}\, |G;0,0;G\rangle$$
$$= - t^4 \sum_{k\in L}\sum_{p\in R} \frac{u_k v_k^* u_q^* v_p}{(E_k-\epsilon)(-2\epsilon)(E_p-\epsilon)}\, |G;\downarrow,\uparrow;G\rangle$$
$$= - \frac{1}{16} J e^{+i\phi}\, |G;\downarrow,\uparrow;G\rangle \ .$$

The path which transfers Cooper pairs from the left to the right superconductor contributes the complex conjugate of the above one.

Adding the contributions of the different paths, we obtain

$$H^{(4)}_{C_1} = 4 \times \frac{J}{16} \times 2\cos\phi \times \begin{bmatrix} 0 & & \\ & -1 & +1 \\ & +1 & -1 \\ & & & 0 \end{bmatrix} = J\cos\phi \left[\mathbf{S}_a \cdot \mathbf{S}_b - \frac{1}{4} \right] \ . \tag{46}$$

References

1. See, e.g., *Mesoscopic Electron Transport*, edited by L. L. Sohn, L. P. Kouwenhoven, and G. Schön (Kluwer, Dordrecht, 1997).
2. I. O. Kulik, Sov. Phys. JETP **22**, 841 (1966); H. Shiba and T. Soda, Prog. Theor. Phys. **41**, 25 (1969); L. N. Bulaevskii, V. V. Kuzii, and A. A. Sobyanin, JETP Lett. **25**, 290 (1977).

3. L. I. Glazman and K. A. Matveev, Pis'ma Zh. Eksp. Teor. Fiz. **49**, 570 (1989) [JETP Lett. **49**, 659 (1989)]; B. I. Spivak and S. A. Kivelson, Phys. Rev. B **43**, 3740 (1991).
4. D. C. Ralph, C. T. Black, and M. Tinkham, Phys. Rev. Lett. **74**, 3241 (1995).
5. C. B. Whan and T. P. Orlando, Phys. Rev. B **54**, R5255 (1996); A. Levy Yeyati, J. C. Cuevas, A. Lopez-Davalos, and A. Martin-Rodero, Phys. Rev. B **55**, R6137 (1997).
6. S. Ishizaka, J. Sone, and T. Ando, Phys. Rev. B **52**, 8358 (1995); A. V. Rozhkov and D. P. Arovas, Phys. Rev. Lett. **82**, 2788 (1999); A. A. Clerk and V. Ambegaokar, Phys. Rev. B **61**, 9109 (2000).
7. K. A. Matveev *et al.*, Phys. Rev. Lett. **70**, 2940 (1993).
8. R. Bauernschmitt, J. Siewert, A. Odintsov, and Yu. V. Nazarov, Phys. Rev. B **49**, 4076 (1994).
9. R. Fazio, F. W. J. Hekking, and A. A. Odintsov, Phys. Rev. B **53**, 6653 (1996).
10. J. Siewert and G. Schön, Phys. Rev. B **54**, 7424 (1996).
11. D. Loss and D. P. DiVincenzo, Phys. Rev. A **57**, 120 (1998).
12. D. Loss and E. V. Sukhorukov, Phys. Rev. Lett. **84**, 1035 (2000).
13. M.-S. Choi, C. Bruder, and D. Loss, Phys. Rev. B **62**, 13569 (2000).
14. P. Recher, E. V. Sukhorukov, and D. Loss, cond-mat/0009452.
15. A. Auerbach, *Interacting Electrons and Quantum Magnetism* (Springer-Verlag, Berlin, 1994).
16. See, e.g., M. Tinkham, *Introduction to Superconductivity*, 2nd ed. (McGraw-Hill, New York, 1996).
17. D. Vollhardt and P. Wölfle, *The Superfluid Phases of* ^{3}*He* (Taylor and Francis, London, 1990).
18. G. M. Luke *et al.*, Nature **394**, 558 (1998).
19. J. M. Kikkawa and D. D. Awschalom, Phys. Rev. Lett. **80**, 4313 (1998).
20. B. J. van Wees and H. Takayanagi, in [1]; H. Takayanagi, E. Toyoda, and T. Akazaki, Superlattices and Microstructures **25**, 993 (1999); A. Chrestin *et al.*, ibid., 711 (1999).